Journal of Ceramic Processing Research. Vol. 17, No. 4, pp. 389~393 (2016)

J O U R N A L O F
Ceramic Processing Research

Structural and electrochemical properties of anodic aluminum oxide based electrolyte-insulator-metal device according to the heat treatment

Seo-Hyeon Jo, Sung-Gap Lee* and Jin-Ho Yeo

Department of Ceramic Engineering, Eng. Res. Insti., Gyeongsang National University, Jjinjudaero 501, 660-701, Jinju, South Korea

In this study, we fabricated the electrolyte-insulator-metal sensor on the base of Si_3N_4 film-coated AAO template with variation of the heat treatment time. The structural and electrochemical properties of AAO sensor were investigated for applications in chemical sensors. Si_3N_4 layer was uniformly coated with the thickness of about 10 nm. Alumina layer, heat-treated for 10 h, crystallized from the amorphous phase to crystalline phase of γ-Al_2O_3, and the spacing of lattice plane of the oxide layer was about 2.638 Å. The AAO sensor heat-treated for 10 h showed the good normalized C-V properties, and the set values of the capacitance and the pH sensitivity were –0.3 V and 54.1 mV/pH, respectively.

Key words: Anodic Aluminium Oxide, Crystallization, capacitive EIS, biosensor.

Introduction

The anodic aluminium oxide (AAO) template is known for playing important role in the fabrication of 1D nanostructure, including nanotubes, nanowires made of various materials [1-3]. AAO template consists of a close-packed array of hexagonal cells, each containing a central pore and it is advantage which the pore size and the interval between pores can be easily controlled by appropriately anodizing conditions, such as electrolyte, voltage, time and temperature [4-6]. In addition, AAO template has advantages such as good chemical and thermal stability [7-10]. Therefore, using the characteristics of AAO template, many studies have been conducted for application of supercapacitors or sensors. The ion-sensitive field-effect transistors (ISFETs) are an electrochemical sensor that reacts to ionic activity at the electrolyte/membrane interface of exposed gate window. However, pH-ISFET devices up to now have been limited to biomedical applications due to the necessity of a corrosion-resistant encapsulation of the electrical connections against the surrounding liquid [11]. To overcome these drawbacks, many researchers have studied the chemical sensor of simple capacitive electrolyte-insulator-semiconductor (EIS) structure, which is corresponded to the gate region of an ISFET [Ref]. Recently, the structured or porous silicon structures with the large active sensor surface have been studied for miniaturization and high performance of the capacitive EIS sensors [12].

In this work, a new concept for potentiometric aluminium-based sensors has been developed using anodic aluminium oxide (AAO) process. This porous electrolyte-insulator-metal (EIM) structure should exhibit several advantages compared to EIS structure: process for forming a lower electrode is not necessary and the production cost is low due to the simple fabrication process. We measured the structural and electrochemical properties of EIM sensors according to the heat treatment of AAO template, and investigated the application as a transducer material for chemical sensors or biosensors.

Experimental

High purity aluminum foils (99.999%, Alfa Aeser) with a thickness of 0.5 mm were used as substrate. Prior to anodization, the metal surfaces were degreased, etched in ethanol solution and rinsed in distilled water, then electropolished to obtain a smooth surface. The first anodizing process was carried out in a 0.04 M oxalic acid at 90 V for 1 h. The first anodized layer was subsequently removed in a mixture of chromic acid and phosphoric acid at 65°C for 3 h. The second anodizing process was carried out in a 0.04 M oxalic acid solution at 90 V for 3 min. After second anodizing process, the pores are widened by etching in a 5 wt% phosphoric acid solution at 45°C for 15 min. And then the heat treatment was carried out under various times in the range of 0-10 hr. Si3N4 film, which used as the sensing layer of sensor devices, was deposited by plasma enhanced chemical vapor deposition (PECVD) technique onto the porous AAO templates. AAO templates were characterized by using X-ray diffraction (XRD) and transmission electron microscopy (TEM). For pH measurements, technical buffer solutions (Titrisol Merk) of pH 4-10 were used. In order to examine the potentiometric response of the sensors, the prepared samples can be easily mounted in a home-made measuring cell sealed by an O-ring. The

*Corresponding author:
Tel : +0557721687
Fax: +0557721689
E-mail: lsgap@gnu.ac.kr

sensor was contacted on its front side by the electrolyte and an Ag/AgCl reference electrode, on the rear side by a gold-plated pin. To study the sensor characteristics, capacitance/voltage (C/V) measurements were performed with LCR meter (Fluke PM 6306). And for verify the potential to biosensor the voltage was investigated with various pH solutions using Data acquisition/Switch unit (Agilent, 34970A).

Results and Discussion

Measurements of the differential thermal analysis (DTA) and the thermogravimetry (TG) curves of the porous alumina powder were conducted, and the results are shown in Fig. 1.

An endothermic peak due to the decomposition of aluminium hydroxide was observed in the temperature range of 150 ºC to 220 ºC (in heating graph) [13]. The weight loss at around 420 ºC was about 1.34% and was attributed to the combustion of impurities, which were entered in the process of separation into the porous alumina from AAO template. Considering the endothermic curve at around 250 ºC in the cooling process, the heat treatment temperature was determined by 270 ºC.

Fig. 2 shows the X-ray diffraction pattern of AAO template with variation of the heat treatment time. The peak of aluminium hydroxide was observed at around 38 º in the specimen carried out the heat treatment for 1 h. However, AAO template, heat-treated for more than 5 h, showed the typical polycrystalline structure and a single phase of γ-Al_2O_3 (JCPDS No. 01-075-0921). The average crystal size of AAO template, heat-treated for 10 h, was estimated to be about 46 nm from the broadening of the corresponding XRD peaks using the Scherrer formula [14].

For more detailed investigation on the microstructure of the Si_3N_4 film-coated AAO template with variation of the heat treatment time, a TEM study was performed. All Si_3N_4 layers were uniformly coated with the thickness of about 10 nm, and pore wall as well as the pore bottom is completely covered with Si_3N_4/Al_2O_3 layer sequence, as shown in Fig. 3 and 4.

Fig. 3(a) shows a cross-sectional TEM image of Si_3N_4 film-coated AAO template before heat treatment. In Chen's [15] research, the AAO layer formed in acid solutions at less than approximately 100 V are usually considered to be completely amorphous phase. And heat

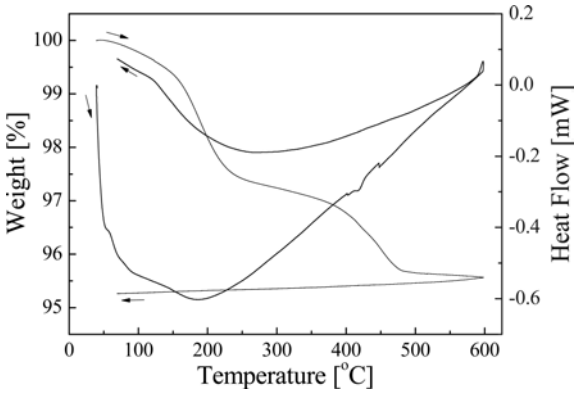

Fig. 1. DTA/TG curves of the alumina powder fabricated by AAO process.

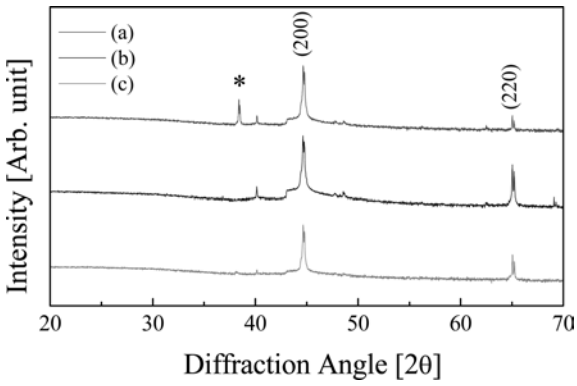

Fig. 2. The X-ray diffraction pattern of the AAO template with heat treatment time: (a) 1 h, (b) 5 h and (c) 10 h.

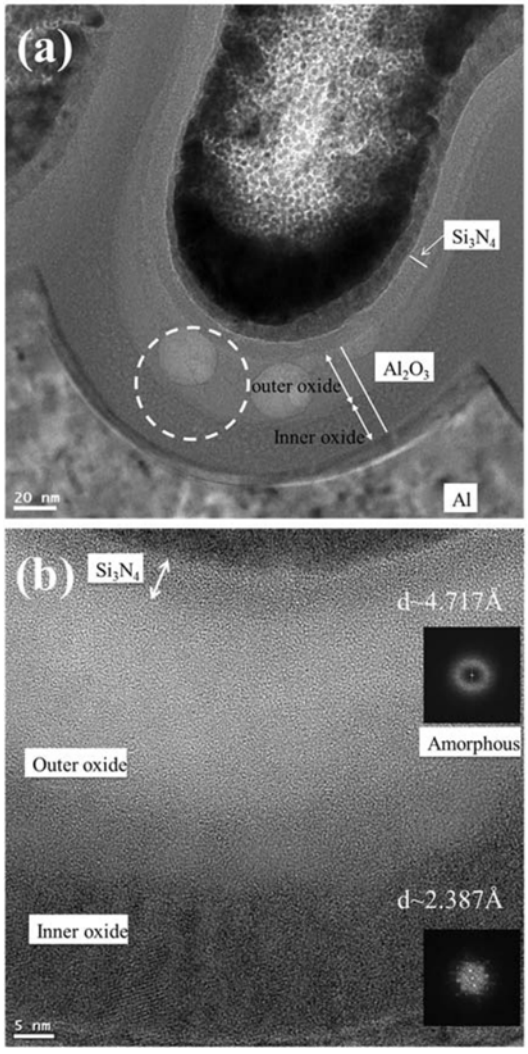

Fig. 3. (a) Cross-sectional TEM micrograph and (b) selected area electron diffraction pattern of cross-sectional image of the Si_3N_4 film-coated AAO template before heat treatment.

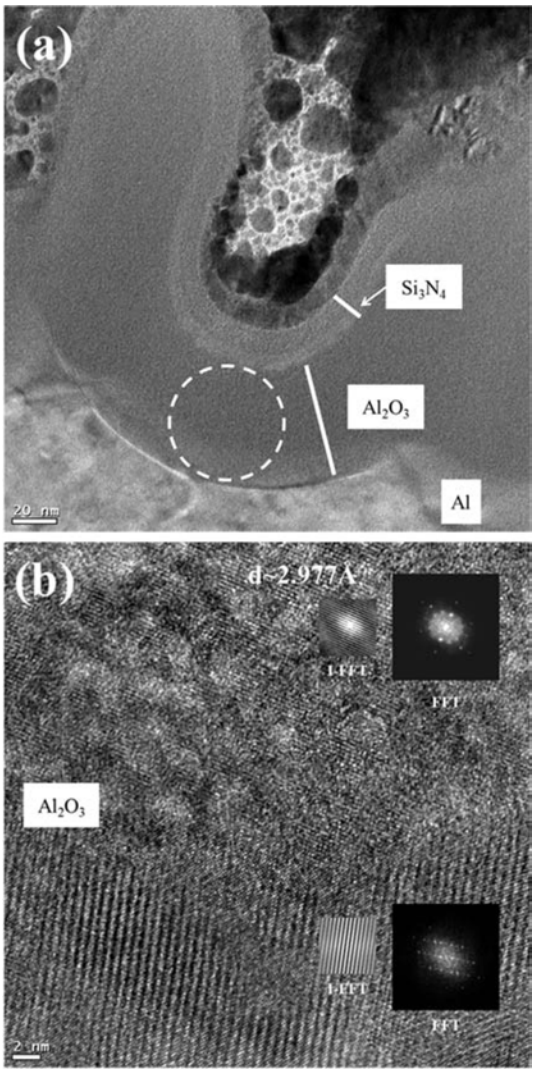

Fig. 4. (a) Cross-sectional TEM micrograph and (b) selected area electron diffraction pattern of cross-sectional image of the Si_3N_4 film-coated AAO template heat-treated for 10 h.

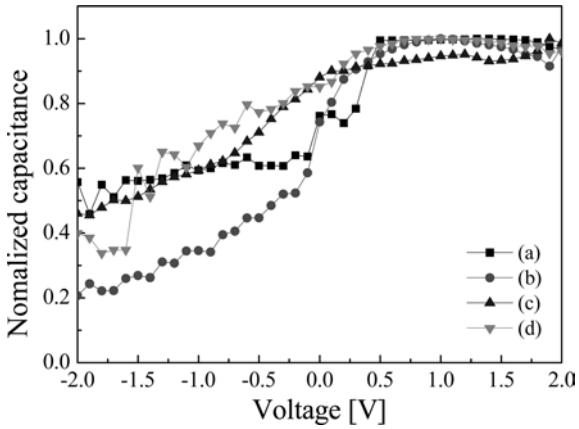

Fig. 5. Normalized capacitance-voltage properties of AAO sensor with variation of the heat treatment time: (a) 0 h, (b) 1 h, (c) 5 h and (d) 10 h.

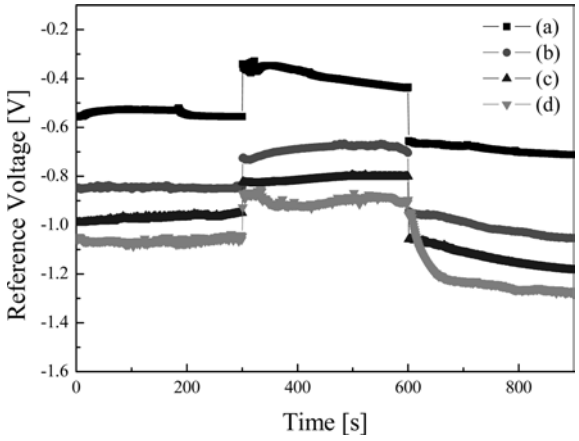

Fig. 6. Hysteresis behavior of AAO sensor with variation of the heat treatment time: (a) 0 h, (b) 1 h, (c) 5 h and (d) 10 h.

treatment is a method that induces AAO crystallization and the stabilization of the nanostructure. In Choi's[16] research, in the AAO process, Al_2O_3 layer was composed of an inner oxide layer formed with pure alumina oxide and an outer oxide layer formed with an anion-contaminated alumina. In this study, Al_2O_3 layer was composed of an inner oxide layer and an outer oxide layer, as shown in Fig. 3(a). The thickness of inner oxide layer and outer oxide layer of the bottom part were about 24 nm and 30 nm, respectively. Fig. 3(b) shows the selected area electron diffraction (SAED) pattern of the cross-sectional image of interface between the AAO template and the Al substrate. The appearance of spot-pattern in the diffraction pattern obtained from the outer oxide layer and inner oxide layer indicated the amorphous phase and crystalline phase, respectively. The spacing of lattice plane of the inner oxide layer was about 2.387 Å.

Fig. 4 shows a cross-sectional TEM image of Si_3N_4 film-coated AAO template heat-treated for 10 h. AAO template is homogeneously covered with the alumina and the Si_3N_4 layer. Especially, by the heat treatment, alumina layer crystallized from the amorphous phase to crystalline phase of γ-Al_2O_3, as shown in Fig. 4(b). This is because the decrease of defects and the diffusion of Al and O ions [15]. The spacing of lattice plane of the oxide layer heat-treated for 10 h was about 2.977 Å.

Fig. 5 shows the normalized capacitance-voltage (C-V) characteristics of AAO sensor with variation of the heat treatment time. C-V measurements were performed with a LCR-meter at a dc voltage which was swept from –2 V to 2 V in steps on 100 mV and a superposed ac voltage with a frequency of 120 Hz and a signal amplitude of 50 mV. The C-V curves have a linear shape, which guarantees that only the concentration-dependent potential shift as resulting chemical sensor is measured [17]. Therefore, the change of capacitance value at the linear region corresponds to the pH-sensitivity property of AAO sensor. The AAO sensor heat-treated for 10 h showed the good normalized C-V properties, and the set values of the capacitance,

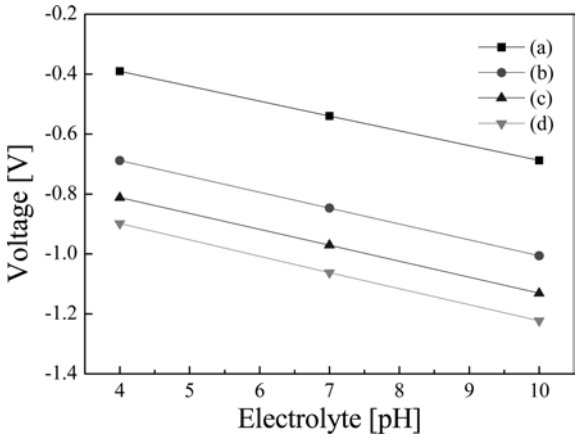

Fig. 7. Characteristic pH calibration curves of AAO sensor with variation of the heat treatment time: (a) 0 h, (b) 1 h, (c) 5 h and (d) 10 h.

working point, of these devices were −0.3 V.

Fig. 6 shows the hysteresis behaviour of AAO sensors with variation of the heat treatment time. The measurement of hysteresis behaviour was performed by immersing the prepared sensors in each pH standard solution for up to 5 min in a set cycle of pH 7 → pH 4 → pH 10. The pH sensitivity of AAO sensors increased with an increase the heat treatment time due to the increase in the crystallinity of alumina layer. The AAO sensor with the heat treatment time of 0 h, 1 h, 5 h and 10 h showed the pH sensitivity of 49.5 mV/pH, 52.9 mV/pH, 53.1 mV/pH and 54.1 mV/pH, respectively.

Fig. 7 shows the corresponding pH calibration curves with variation of the heat treatment time. To determine the pH sensitivity, the pH-dependent shift of the C-V curve was evaluated as the 80% value of the maximum capacitance. As can be seen from the calibration graph in Fig. 7, the linearity characteristics increased with increasing the heat treatment time. For the AAO sensor heat-treated for 10 h, an average pH sensitivity of about 54.1 mV/pH is calculated in the concentration range from pH 4 to pH 8 which is very close to the theoretical Nernstian slope of 58 mV/pH at standard conditions.

Conclusions

Si_3N_4 film coated-AAO templates were fabricated with variation of the heat treatment time. The structural and electrochemical properties were observed for application as chemical sensors. Temperature of the decomposition of aluminium hydroxide was about 200 °C, obtained by DTA/TG analysis. AAO template, heat-treated for more than 5 h, showed the typical polycrystalline structure and a single phase of γ-Al_2O_3. Al_2O_3 layer before the heat treatment was composed of an inner oxide layer and an outer oxide layer, and the outer oxide layer indicated the amorphous phase. But the layer heat-treated for 10 h showed the homogeneously crystallized alumina layer. The pH sensitivity and the linearity characteristics of AAO sensors increased with an increase the heat treatment time due to the increase in the crystallinity of alumina layer.

Acknowledgements

This research was supported by the Pioneer Research Center Program through the National Research Foundation of Korea funded by the Ministry of Education, Science and Technology (2011-0001704).

References

1. H. Masuda, M. Satoh. Fabrication of gold nano dot array using anodic porous alumina as an evaporation mask. Jpn. J. Appl. Phys. 35 (1996) L126-L129.
2. H. Masuda, H. Yamada, M. Satoh, H. Asoh, M. Nakao, T. Tamamura. Highly ordered nanochannel-array architecture in anodic alumina. Appl. Phys. Lett. 71 (1997) 2770-2772.
3. E. Moyen, H. Sahaf, M. Mace, L. Masson, K. Sengupta, M. Hanbucken. Novel anodic aluminum oxide-based nanofabrication: applications in physics and biology. Surf. Interface Anal. 42 (2010) 1556-1560.
4. H. Masuda, F. Hasegwa, S. Ono. Self-ordering of cell arrangement of anodic porous alumina formed in sulfuric acid solution. J. Electrochem. Soc. 144 (1997) L127-L130.
5. S. Z. Chu, K. Wada, S. Inoue, M. Isogai, A. Yasumori. Fabrication of ideally ordered nanoporous alumina films and integrated alumina nanotubule arrays by high-field anodization. Adv. Mater. 17 (2005) 2115-2119.
6. M. A. Kashi, A. Ramazani, Y. Mayamai, M. Noormohammadi. Fabrication of self-ordered nanoporous alumina with 69-115 nm interpore distances in sulfuric/oxalic acid mixtures by hard anodization. Jpn. J. Appl. Phys. 49 (2010) 015202.
7. A. M. Md Jani, D. Losicc, N. H. Voelcker. Nanoporous anodic aluminium oxide: advances in surface engineering and emerging applications. Progress in Materials Science 58 (2013) 636-704.
8. S. Iijima. Helical microtubules of graphitic carbon. Nature 354 (1991) 56-58.
9. C.Sunseri, C. Spadaro, S. Piazza, M. Volpe, F. Di Quarto. Porosity of anodic alumina membranes from electrochemical measurements. J. Solid State Electrochem. 10 (2006) 416-421.
10. G. Hu, H. Zhang, W. Di, T. Zhao. Study on wet etching of AAO template. Appl. Phys. Res. 1 (2009) 78-82
11. B. H. van der Schoot, P. Bergveld. ISFET based enzyme sensors. Biosensors 3 (1987/1988) 161-186
12. M. J. Schöning, A. Kurowski, M. Thust, P. Kordos, J.W. Schultze, H. Lüth. Capacitive microsensors for biochemical sensing based on porous silicon technology. Sensors and Actuators B 64 (2000) 59-64
13. I. Chen, S. Hwang, S. Chen. Ind. Eng. Chem. Res. Chemical kinetics and reaction mechanism of thermal decomposition of aluminum hydroxide and magnesium hydroxide at high temperature (973-1123 K). 28 (1989) 738-742
14. Cullity B. Elements of X-ray Diffraction, M A:Addison-Wesley 1978.
15. C. C. Chen, J. H. Chen, C. G. Chao. Post-treatment method of producing ordered array of anodic aluminium oxide using general purity commercial (99.7%) aluminium. Jap. J. Appl. Phys. 44 (2005) 1529-1533.

16. J. Choi. Ph. D dissertation, Martin-Luther-Universität, Halle-Wittenberg, Germany (2004).
17. M. Schoning, M. Arzdorf, P. Mulchandaui, W. Chen, A. Mulchandani. A capacitive field-effect sensor for the direct determination of organophosphorus pesticides. Sensors and Actuators B 91 (2003) 92-97.